

BMB Reports – Manuscript Submission

Manuscript Draft

Manuscript Number: BMB-16-197

Title: Celecoxib-mediated activation of endoplasmic reticulum stress induces de novo ceramide biosynthesis and apoptosis in hepatoma HepG2 cells

Article Type: Article

Keywords: ceramide; apoptosis; celecoxib; sphingolipid; ER stress

Corresponding Author: Tae-Sik Park

Authors: Hyo Jin Maeng¹, Jae-Hwi Song¹, Goon-Tae Kim¹, Yoo-Jeong Song¹, Kangpa Lee², Jae-Young Kim¹, Tae-Sik Park^{1,*}

Institution: ¹Department of Life Science, Gachon University,
²Department of Physiology, Konkuk University,

Manuscript Type: Article

Title: Celecoxib-mediated activation of endoplasmic reticulum stress induces *de novo* ceramide biosynthesis and apoptosis in hepatoma HepG2 cells

Author's name: Hyo Jin Maeng^{1,3}, Jae-Hwi Song^{1,3}, Goon-Tae Kim¹, Yoo-Jeong Song¹, Kangpa Lee², Jae-Young Kim¹, Tae-Sik Park^{1*}

Affiliation: ¹Department of Life Science, Gachon University, Sunghnam, 461-701, Korea. ²Department of Physiology, Konkuk University, School of Medicine, Seoul 143-701, Korea.

Running Title: Celecoxib activates ER stress and apoptosis.

Keywords: ceramide, apoptosis, celecoxib, sphingolipid, ER stress

Corresponding Author's Information: Tel: +82-1027575903, Fax: +82-317508573, E-mail: tspark@gachon.ac.kr.

ABSTRACT

Ceramides are the major sphingolipid metabolites involved in cell survival and apoptosis. When HepG2 hepatoma cells were treated with celecoxib, the expression of the genes in *de novo* sphingolipid biosynthesis and sphingomyelinase pathway was upregulated and cellular ceramide was elevated. In addition, celecoxib induced endoplasmic reticulum (ER) stress in a time-dependent manner. SPTLC2, a subunit of serine palmitoyltransferase, was overexpressed by adenovirus. Adenoviral overexpression of SPTLC2 (AdSPTLC2) decreased cell viability of HEK293 and HepG2 cells. In addition, AdSPTLC2 induced apoptosis via the caspase-dependent apoptotic pathway and elevated cellular ceramide, sphingoid bases, and dihydroceramide. However, overexpression of SPTLC2 did not induce ER stress. Collectively, celecoxib activates *de novo* sphingolipid biosynthesis and the combined effects of elevated ceramide and transcriptional activation of ER stress induce apoptosis. However, activation of *de novo* sphingolipid biosynthesis does not activate ER stress in hepatoma cells and is distinct from the celecoxib-mediated activation of ER stress.

INTRODUCTION

Ceramide is a component of the plasma membrane and a bioactive signaling molecule involved in regulating cellular events including cell cycle arrest, apoptosis, senescence, and stress responses (1). Ceramide can be produced from the *de novo* pathway and the sphingomyelinase pathway via sphingomyelinase (2). Formation of ceramide is induced by tumor necrosis factor- α (TNF- α), Fas ligand, oxidative stress, heat stress, and chemotherapeutics (3-5). The balance of ceramide and sphingosine 1-phosphate (S1P), a sphingolipid metabolite that induces cell proliferation, is called “sphingolipid rheostat” and is known to determine cell fate (6).

Chemotherapeutic agents induce ceramide synthesis via activation of dihydroceramide desaturase or activation of *de novo* pathways (7, 8). Celecoxib, an inhibitor of cyclooxygenase 2 (COX2), induces cell cycle arrest and apoptosis in various cancer cells including colon, lung and cervical cancers (9-11). In addition to its inhibitory effect on COX2, celecoxib activates modulatory effects on sphingolipid biosynthesis and elevates cellular ceramide (12). Celecoxib-mediated ceramide elevation activates signaling proteins such as cathepsin D, protein kinase ζ , and protein phosphatase-1 and contributes to the progression of apoptotic events (13).

The endoplasmic reticulum (ER) is the organelle responsible for protein folding, lipid synthesis, and protein maturation. ER stress is induced by the accumulation of unfolded proteins in the ER lumen, leading to activation of the unfolded protein response and the transcriptional upregulation of chaperones (14). Various studies have demonstrated that ER stress leads to growth arrest and apoptosis in carcinoma cells (15, 16). Fumonisin B1, a ceramide synthase (CerS) inhibitor, inhibits ceramide-induced ER stress and alteration of ceramide synthase 6 (CerS6) up-regulates the activating transcription factor 6 (ATF6)-CCAAT-enhancer-binding protein homologous protein (CHOP) pathway and apoptosis in human head and neck squamous cell carcinomas (17, 18). However, activation of ER stress and sphingolipid synthesis by celecoxib in hepatoma cells has remained unexplored.

The present studies were to determine whether celecoxib is a transcriptional activator of *de novo* sphingolipid biosynthesis and induces ceramide-mediated apoptosis in hepatoma cells. Furthermore, we examined whether activated *de novo* sphingolipid biosynthetic pathway mediates elevation of cellular ceramide regulates ER stress. Collectively, the results identified the apoptotic effects of celecoxib on hepatoma cells via the

activation of ceramide synthesis and ER stress.

UNCORRECTED PROOF

RESULTS

Celecoxib transcriptionally upregulates *de novo* sphingolipid biosynthetic genes and elevates sphingolipid metabolites

Celecoxib is implicated in the elevation of cellular sphingolipids (12). Therefore, we investigated whether celecoxib transcriptionally upregulates SPTLC1 and SPTLC2. SPTLC1 and SPTLC2 are the two major subunits of serine palmitoyltransferase (SPT), which is the first and rate-limiting step of the sphingolipid biosynthetic pathway. We treated HepG2 cells with celecoxib at various time points. Eighty μM of celecoxib was chosen for this study because of maximum inducing effect (data not shown). The expression of SPTLC1 and SPTLC2 mRNA and proteins was upregulated by celecoxib and SPT activity increased two-fold (Figure 1A-C). To determine whether celecoxib alters the transcription of other sphingolipid biosynthetic genes, we measured the expression of genes in the *de novo* and sphingomyelinase pathways. We found that all ceramide synthase 1, 2, 3, 5, 6, alkaline ceramidases 2-3, acid ceramidase, and neutral ceramidase were upregulated in a time-dependent manner (Figure 1D). However, the expression of dihydroceramide desaturase, sphingosine kinase 2, and ceramide synthase 4 was not altered. In addition, sphingomyelinases were

also upregulated in a time-dependent manner (Figure 1D). These results suggest that celecoxib-mediated ceramide elevation was due to the transcriptional activation of both the *de novo* and sphingomyelinase pathways.

Transcriptional activation of ceramide biosynthesis by celecoxib implies that sphingolipids would be elevated in HepG2 hepatoma cells. To assess this, we measured sphingolipids in HepG2 cells by LC/MS/MS after treatment with celecoxib at various time points. Total ceramide levels were elevated by celecoxib. The levels of long chain ceramides, including C16:0 and C18:0 ceramide, were elevated in a time-dependent manner, but the levels of very long chain ceramides, including C24:0 and C24:1 ceramide, were not changed (Figure 1E). Sphinganine and sphingosine were elevated but S1P was not altered (Figure 1F). In addition, all dihydroceramides were increased in a time-dependent manner (Figure 1G). In contrast, sphingomyelin levels were not altered by celecoxib (Figure 1H). These findings indicate that celecoxib-mediated induction of sphingolipid biosynthetic genes leads to the activation of *de novo* sphingolipid biosynthesis and the elevation of sphingolipid levels. Increased levels of

cytotoxic long chain ceramides implicate celecoxib in the production of apoptotic long chain ceramide and the initiation of apoptotic events

Celecoxib activates ER stress in HepG2 hepatoma cells

Next, we tested whether celecoxib activates ER stress in HepG2 cells. When we treated cells with celecoxib, mRNA levels of ATF4, ATF6, spliced XBP1 (sXBP1), GRP78, and CHOP were upregulated in a time-dependent manner (Figure 2A-E). We also found that celecoxib increased the protein levels of ATF4, ATF6, sXBP-1, unspliced XBP1 (uXBP1), and CHOP until 6 h post-treatment (Figure 2F). After 12 h, celecoxib-induced expression of these proteins disappeared, probably due to the combined cytotoxic effects of celecoxib and ceramide-mediated apoptotic events. Interestingly, ATF6 and CHOP remained elevated until 12 h post-treatment (Figure 2F). These results suggest that celecoxib is responsible for the activation of ER stress in HepG2 hepatoma cells.

Adenoviral expression of SPTLC2 is cytotoxic and elevates cellular ceramide

The finding that celecoxib activates *de novo* sphingolipid biosynthesis and ER stress prompted us to distinguish celecoxib-dependent events from ceramide effects. For this, we constructed adenoviruses containing SPTLC1 (AdSPTLC1) and SPTLC2 (AdSPTLC2), which are the major subunits of SPT, the first and rate-limiting step in sphingolipid biosynthesis. During adenovirus production in HEK293 cells, SPTLC1 did not affect the adenovirus yield and followed the regular processes of adenovirus production. However, SPTLC2 causes cell death and low adenovirus yield (Figure 3A). When we treated HepG2 cells with these adenoviruses, SPTLC1 or SPTLC2 protein levels were significantly elevated (Figure 3B). Adenoviral infection did not affect 24 h cell viability. AdSPTLC2 infection reduced cell viability by 51% within 48 h (Figure 3C). In contrast, AdSPTLC1 infection did not affect cell viability. To investigate whether SPTLC2 overexpression activates the *de novo* ceramide biosynthesis pathway, we measured sphingolipid metabolites by LC/MS/MS in HepG2 cells after AdSPTLC1 or AdSPTLC2 infection. Ceramide, sphinganine, sphingosine, and dihydroceramide levels in AdSPTLC2-treated HepG2 cells were higher in cells infected with AdSPTLC2 than in those infected with AdGFP or AdSPTLC1 (Figure 3D-F). However, sphingosine 1-phosphate and sphingomyelin (SM) levels were not altered by AdSPTLC1 or 2 (Figure

3E, G). Additionally, inconsistent with the celecoxib results, the levels of long chain and very long chain ceramides increased (Figure 1). These findings indicate that SPTLC2 expression is cytotoxic due to ceramide accumulation.

Activation of de novo sphingolipid biosynthesis by SPTLC2 overexpression induces apoptosis but not ER stress

We treated HepG2 hepatoma cells with AdSPTLC viruses to determine if SPTLC2-mediated cytotoxicity is due to ceramide-mediated apoptosis. Cell morphology was not altered by AdSPTLC1, but AdSPTLC2 infection caused apoptotic morphology after 24 h of infection (Figure 4A). To confirm this, the proportions of apoptotic cells were analyzed by flow cytometry. Apoptosis was significantly increased by AdSPTLC2 infection (66.1% of cells in apoptotic phase), compared to 22.43% or 31.48% of AdGFP or Ad-SPTLC1 infected cells in the apoptotic phase, respectively (Figure 4B). Interestingly, the proportion of apoptotic cells was slightly higher after AdSPTLC1 infection than after AdGFP infection. This is probably due to increased SPTLC1 supply to the SPT complex. In addition, cleavage of caspase 9 and PARP and decreased caspase 3 were only found in the AdSPTLC2 treatment (Figure 4C). Furthermore, adenoviral overexpression of SPTLC1 or SPTLC2 increased SPT enzyme activity by 3.7- and 9.2-fold,

respectively (Figure 4D). These results indicate that overexpression of SPTLC2, a catalytic subunit of SPT, is implicated in caspase-dependent apoptotic events.

The fact that celecoxib activates ER stress suggests that it may be activated by increased ceramide. To confirm this, we infected cells with adenoviruses and examined transcriptional expression of ER stress markers. However, we did not find any change in ER stress markers including ATF4, ATF6, sXBP1, GRP78, and CHOP (Figure 4E). Only SPTLC1 overexpression upregulated CHOP 1.6-fold. These results suggest that activation of *de novo* sphingolipid biosynthesis, represented by SPTLC2 overexpression, induces apoptosis via ceramide accumulation but not via ER stress.

DISCUSSION

Sphingolipids are major components of eukaryote cells that play important roles in biological processes. Ceramide is an important metabolic intermediate in the sphingolipid biosynthetic pathway and regulates cell proliferation and apoptosis (19). The elevation of cellular ceramide levels is caused by the activation of the *de novo* synthetic pathway or the sphingomyelin salvage pathway (20). Based on previous results that celecoxib activates sphingolipid synthesis, our study demonstrated that: 1) celecoxib transcriptionally upregulates the expression of *de novo* ceramide biosynthetic genes and the sphingomyelinase pathway; 2) activation of the *de novo* ceramide biosynthetic pathway induces apoptosis via activation of the caspase cascade; and 3) celecoxib activates ER stress in hepatoma cells but ceramide accumulation does not.

Celecoxib is a therapeutic medicine used to manage pain and inflammation in osteoarthritis and rheumatoid arthritis (21). Celecoxib is a selective COX2 inhibitor and nonsteroidal anti-inflammatory drug and inhibits the production of prostaglandins, such as PGI₂, PGF_{2α}, PGD₂, and PGE₂, preventing inflammatory responses in joints and bone (22, 23). Previous reports have demonstrated that only celecoxib among coxib-class drugs

specifically increases the cellular levels of dihydroceramide and/or ceramide in HCT-116 colon cancer cells (24). This result suggest that celecoxib-mediated increased ceramide and dihydroceramide are associated with increased levels of apoptosis. Treatment of HepG2 hepatoma cells with celecoxib upregulated the expression of genes in the *de novo* ceramide biosynthetic pathway. In addition, sphingomyelinases, which generate ceramide from sphingomyelin, were also upregulated (Figure 1A). Interestingly, sphingolipid profiling results showed that long chain ceramides, including C16- and C18-ceramide, were increased by celecoxib. In contrast, the levels of very long chain ceramides, such as C24-, C24:1-ceramide, were not altered. Since long chain ceramides are pro-apoptotic and the very long chain ceramides are associated with cell proliferation, these results suggest that apoptosis is induced by an increased proportion of long chain ceramide species (25-27). These results suggest that alteration of specific ceramide levels and proportion modulates pre-apoptotic events aroused by celecoxib.

Since both *de novo* and sphingomyelinase pathways are involved in ceramide production, we first examined whether the *de novo* pathway contributes to increased apoptosis. When SPT subunits were expressed by

adenoviral infection, only the morphology of AdSPTLC2-infected cells was altered, and cell survival decreased in time- and gene dose-dependent manner. Given that adenoviral SPTLC1 expression had no effect on cell survival and SPTLC2 expression induced apoptosis it is likely that SPTLC2 is a major catalytic subunit for SPT reaction.

Consistent with the cell viability results, the flow cytometry analyses demonstrated that cells are entering into the apoptotic stage. Indeed, the proportion of apoptotic cells was significantly increased by adenoviral SPTLC2 expression. SPTLC1 overexpression induced a slightly higher amount of apoptosis than did the GFP controls, indicating that the pairing of SPTLC1 and SPTLC2 subunits was increased by elevated levels of SPTLC1 subunit, as shown previously (28, 29). However, endogenous SPTLC2 is limited, resulting in only a slight increase in apoptosis.

The finding that adenoviral expression of SPTLC2 induced cleavage of Caspase-3, -9, and PARP suggest that elevated ceramide causes mitochondrial intrinsic pathway-dependent apoptosis. We found that celecoxib activates the regulatory transcription factors in ER stress in HepG2 hepatoma cells. Expression of XBP1, ATF4, ATF6, and CHOP was gradually upregulated by celecoxib in a time-dependent manner and altered the cell

status from normal stage to apoptotic progression. However, adenoviral SPTLC2 expression and activation of *de novo* ceramide biosynthesis did not affect the expression of transcription factors in ER stress (Figure 4). These results indicate that elevated endogenous ceramide is not associated with activation of ER stress in these hepatoma cells. Thus, the involvement of the sphingomyelinase pathway in apoptotic progression deserves further study.

Taken together, our studies identified the roles of *de novo* ceramide biosynthetic pathway in celecoxib-mediated ceramide increase and apoptosis. This observation is relevant to stress-induced apoptosis based on the sensitivity of cancer cells. This suggests a novel strategy to synergize the anti-cancer activity of celecoxib. Further studies will define proper combination therapies by enhancing the efficacy of anti-cancer treatments with celecoxib, or by modulation of ceramide synthesis in liver cancer.

MATERIALS AND METHODS

Cell culture

HepG2 hepatoma cells were obtained from the American Type Culture Collection (ATCC). The cells were cultured in Dulbecco's modified Eagle medium (DMEM; WelGENE) supplemented with 10% fetal bovine serum (FBS), 1 U/ml penicillin, and 1 µg/ml streptomycin and incubated at 37°C in a 5% CO₂ atmosphere.

Cell viability

HepG2 cells seeded on 96-well plates were treated with celecoxib or adenoviruses for 24 and 48 h. Then, cell viability was assessed using the XTT colorimetric solution (WelGENE).

Adenovirus construction

SPTLC1 and SPTLC2 recombinant adenoviruses (AdSPTLC1, AdSPTLC2) were constructed using an AdEasy Adenoviral Vector System (Stratagene) and a pAdTrack CMV vector as described previously (30). As a control, adenovirus expressing green fluorescence protein (AdGFP) was prepared as described above.

Flow cytometric analysis of apoptosis

HepG2 cells were infected with each adenovirus for 24 h. Cells were double-stained with propidium iodide and Annexin V according to the manufacturer's instructions (Annexin V-FITC Apoptosis Detection Kit I; BD Biosciences) and analyzed using a FACS Calibur flow cytometer (BD Biosciences) and FlowJo software (Tree Star).

Western blot

Cells were collected and lysed in lysis buffer (20 mM Tris-HCl, pH 7.5, 5 mM EDTA, 100 mM NaF, 10 mM $\text{Na}_2\text{P}_2\text{O}_7$, 2 mM Na_3VO_4 , 1% Triton X-100, protease inhibitor) by vortexing. Thirty micrograms of protein lysate was subjected to 10% SDS-polyacrylamide gel electrophoresis followed by immunoblotting analyses. Antibodies were used to detect caspase-9, caspase-3, PARP (Cell signaling Technology), XBP-1, ATF4, CHOP (Santa Cruz Biotechnology), ATF6 (Abcam), and β -actin (Millipore). The blots were detected with enhanced chemiluminescent substrate (Bio-Rad).

RNA extraction and Quantitative Real-Time PCR

Total RNA was isolated from HepG2 cells using the easy-spin (DNA free) Total RNA Extraction Kit (iNtRON) according to the manufacturer's

procedure. Real-Time PCR analysis was performed with StepOnePlus equipment (Applied Biosystems) using SYBR Green Master Mix (Takara). mRNA expression levels were normalized to β -actin. The primers used were shown previously (31).

Sphingolipid analysis by LC/MS/MS

HepG2 cells were lysed in lysis buffer for sphingolipid analysis. C17-ceramide was used as an internal standard. One milligram of protein from was extracted cell lysates using MeOH/CHCl₃ (1:2, v/v). The organic phase was separated and evaporated under N₂. Ceramides (Cer), sphinganine (SA), sphingosine (SO), dihydroceramides (dhCer), and sphingomyelin (SM) were separated by high-performance liquid chromatography using a C18 column (XTerra C18, 3.5 μ m, 2.1 \times 50 mm) and ionized in positive electrospray ionization (ESI) mode as described by Lee *et al* (31, 32). [M+]/product ions from corresponding sphingolipid metabolites were monitored for multiple reaction monitoring (MRM) quantification by a tandem mass spectrometer, API 4000 Q-trap (Applied Biosystems, Framingham, MA), interfaced with ESI.

Statistical analysis

The data are shown as mean \pm SEM. Differences between groups were analyzed by the Student *t* test. $p < 0.05$ was considered significant.

ACKNOWLEDGEMENTS

This research was supported by the Bio and Medical Technology Development Program through the National Research Foundation of Korea (NRF), funded by the Korean government (MSIP) (NRF-2014M3A9B6069338) to T.S.P.

CONFLICT OF INTERESTS

The authors declare that there are no conflicts of interest.

FIGURE LEGENDS

Figure 1. Celecoxib upregulates the expression of sphingolipid biosynthetic genes and elevates cellular sphingolipid levels. HepG2 cells were treated with 80 μ M celecoxib and were harvested at various time points. Expression levels of SPTLC1 and SPTLC2 mRNA (A) and proteins (B) were measured by quantitative real-time PCR and immunoblotting respectively. SPT enzyme activity was measured from the cell lysates at indicated times post-celecoxib treatment (C). Expression of sphingolipid biosynthetic genes was measured as the relative fold-increase, compared to no-treatment controls (D). Sphingolipids from HepG2 cells treated with celecoxib at indicated times were analyzed by LC/MS/MS as described in *Materials and Methods*. Total ceramides (E), sphinganine (SA), sphingosine (SO), and sphingosine 1-phosphate (S1P) (F), dihydroceramide (dhCer) (G), and sphingomyelin (SM) (H) were quantified. Data are presented as the mean \pm SEM. n = 3. *p < 0.05. Amount of mRNA was normalized by β -actin.

Figure 2. Celecoxib upregulates ER stress in HepG2 hepatoma cells. HepG2 cells were harvested at indicated times after celecoxib treatment and

mRNA expression of ER stress markers including ATF4 (A), ATF6 (B), spliced XBP1 (sXBP1) (C), GRP78 (D), and CHOP (E) was measured by quantitative real-time PCR. Amount of mRNA was normalized by β -actin. Data are presented as the mean \pm SEM. n = 3. *p < 0.05. Whole-cell lysates were subjected to immunoblotting analyses of ATF4, ATF6, XBP-1, and CHOP (F). β -actin was used to normalize the mRNA amount.

Figure 3. Adenoviral overexpression of Sptlc2 decreases cell viability in HepG2 cells and elevates cellular sphingolipids. For adenovirus production, HEK293 cells were infected with adenoviruses containing SPTLC1 (AdSPTLC1) and SPTLC2 (AdSPTLC2). Pictures were taken to observe cell morphologies at indicated times post-infection (A). Since GFP is co-expressed with the gene of interest, expression of the gene was observed indirectly with GFP expression. HepG2 cells were infected with adenoviruses containing SPTLC1 or SPTLC2 at 2 MOI (multiplicity of infection) and protein expression was examined by immunoblotting (B). Cell viability was measured by XTT assay after incubation with 2 or 5 MOI of SPTCL1 and SPTLC2 adenoviruses for 24 and 48 h (C). Data are presented as the mean \pm SEM. n = 3 *p < 0.05. Sphingolipids were extracted from

adenoviral infected HepG2 cells after 24 h and analyzed by LC/MS/MS. Total ceramides (D), sphinganine (SA), sphingosine (SO), and sphingosine 1-phosphate (S1P) (E), dihydroceramide (dhCer) (F), sphingomyelin (SM) (G) were quantified. Data are presented as the mean \pm SEM. $n = 3$. * $p < 0.05$ vs. GFP. § $p < 0.05$ vs. SPTLC1.

Figure 4. Adenoviral overexpression of SPTLC2 induces apoptosis in HepG2 cells but does not activate ER stress. HepG2 cells were infected with SPTLC1 or SPTLC2 adenoviruses at 2 MOI for 24 and 48 h. Cell morphology was changed only after infection of SPTCL2 adenovirus (A). After 24 h of infection cells were stained with Annexin V and propidium iodide and the degree of apoptosis quantified by flow cytometry (B). Data are presented as the mean \pm SEM. $n = 3$. * $p < 0.05$. HepG2 cells were infected with adenoviruses at 2 MOI for 24 h and whole-cell lysates were subjected to immunoblotting analyses of caspase-3 (Cas 3), caspase-9 (Cas 9), and PARP (C). β -actin was used as a control. Under the same condition, SPT enzyme activity was measured as described in *Materials and Methods* (D). Then, the expression of ER stress genes including ATF4, ATF6, sXBP1, GRP78, and CHOP was measured by quantitative real-time PCR (E).

Amount of mRNA was normalized by β -actin. Data are presented as the mean \pm SEM. n = 3. *p < 0.05.

REFERENCES

1. Kitatani K, Idkowiak-Baldys J and Hannun YA (2008) The sphingolipid salvage pathway in ceramide metabolism and signaling. *Cell Signal* 20, 1010-1018
2. Menaldino DS, Bushnev A, Sun A et al. (2003) Sphingoid bases and de novo ceramide synthesis: enzymes involved, pharmacology and mechanisms of action. *Pharmacol Res* 47, 373-381
3. Brenner B, Ferlinz K, Grassme H et al. (1998) Fas/CD95/Apo-I activates the acidic sphingomyelinase via caspases. *Cell Death Differ* 5, 29-37
4. Goldkorn T, Balaban N, Shannon M et al. (1998) H₂O₂ acts on cellular membranes to generate ceramide signaling and initiate apoptosis in tracheobronchial epithelial cells. *J Cell Sci* 111 (Pt 21), 3209-3220
5. Jenkins GM, Cowart LA, Signorelli P, Pettus BJ, Chalfant CE and Hannun YA (2002) Acute activation of de novo sphingolipid biosynthesis upon heat shock causes an accumulation of ceramide and subsequent dephosphorylation of SR proteins. *J Biol Chem* 277, 42572-42578
6. Baran Y, Salas A, Senkal CE et al. (2007) Alterations of ceramide/sphingosine 1-phosphate rheostat involved in the regulation of resistance to imatinib-induced apoptosis in K562 human chronic myeloid leukemia cells. *J Biol Chem* 282, 10922-10934
7. Wang H, Maurer BJ, Reynolds CP and Cabot MC (2001) N-(4-hydroxyphenyl)retinamide elevates ceramide in neuroblastoma cell lines by coordinate activation of serine palmitoyltransferase and ceramide synthase. *Cancer Res* 61, 5102-5105
8. Perry DK, Carton J, Shah AK, Meredith F, Uhlinger DJ and Hannun YA (2000) Serine palmitoyltransferase regulates de novo ceramide generation during etoposide-induced apoptosis. *J Biol Chem* 275, 9078-9084
9. Grosch S, Tegeder I, Niederberger E, Brautigam L and Geisslinger G (2001) COX-2 independent induction of cell cycle arrest and apoptosis in colon cancer cells by the selective COX-2 inhibitor celecoxib. *FASEB journal : official publication of the Federation of American Societies for Experimental Biology* 15, 2742-2744
10. Kim HS, Kim T, Kim MK, Suh DH, Chung HH and Song YS (2013) Cyclooxygenase-1 and -2: molecular targets for cervical neoplasia. *J Cancer Prev* 18, 123-134

11. Zhang H, Li Z and Wang K (2014) Combining sorafenib with celecoxib synergistically inhibits tumor growth of non-small cell lung cancer cells in vitro and in vivo. *Oncol Rep* 31, 1954-1960
12. Schiffmann S, Sandner J, Schmidt R et al. (2009) The selective COX-2 inhibitor celecoxib modulates sphingolipid synthesis. *Journal of lipid research* 50, 32-40
13. Truman JP, Garcia-Barros M, Obeid LM and Hannun YA (2014) Evolving concepts in cancer therapy through targeting sphingolipid metabolism. *Biochimica et biophysica acta* 1841, 1174-1188
14. Schroder M and Kaufman RJ (2005) ER stress and the unfolded protein response. *Mutat Res* 569, 29-63
15. Puthalakath H, O'Reilly LA, Gunn P et al. (2007) ER stress triggers apoptosis by activating BH3-only protein Bim. *Cell* 129, 1337-1349
16. Kucuksayan E, Konuk EK, Demir N, Mutus B and Aslan M (2014) Neutral sphingomyelinase inhibition decreases ER stress-mediated apoptosis and inducible nitric oxide synthase in retinal pigment epithelial cells. *Free radical biology & medicine* 72, 113-123
17. Senkal CE, Ponnusamy S, Bielawski J, Hannun YA and Ogretmen B (2010) Antiapoptotic roles of ceramide-synthase-6-generated C16-ceramide via selective regulation of the ATF6/CHOP arm of ER-stress-response pathways. *FASEB journal : official publication of the Federation of American Societies for Experimental Biology* 24, 296-308
18. Senkal CE, Ponnusamy S, Manevich Y et al. (2011) Alteration of ceramide synthase 6/C16-ceramide induces activating transcription factor 6-mediated endoplasmic reticulum (ER) stress and apoptosis via perturbation of cellular Ca²⁺ and ER/Golgi membrane network. *J Biol Chem* 286, 42446-42458
19. Hannun YA and Luberto C (2000) Ceramide in the eukaryotic stress response. *Trends Cell Biol* 10, 73-80
20. Kolesnick R (2002) The therapeutic potential of modulating the ceramide/sphingomyelin pathway. *J Clin Invest* 110, 3-8
21. Hirayama A, Tanahashi N, Daida H et al. (2014) Assessing the cardiovascular risk between celecoxib and nonselective nonsteroidal antiinflammatory drugs in patients with rheumatoid arthritis and osteoarthritis. *Circulation journal : official journal of the Japanese*

Circulation Society 78, 194-205

22. Pereira PA, Trindade BC, Secatto A et al. (2013) Celecoxib improves host defense through prostaglandin inhibition during *Histoplasma capsulatum* infection. *Mediators of inflammation* 2013, 950981
23. Tsuji S, Tomita T, Nakase T, Hamada M, Kawai H and Yoshikawa H (2014) Celecoxib, a selective cyclooxygenase-2 inhibitor, reduces level of a bone resorption marker in postmenopausal women with rheumatoid arthritis. *International journal of rheumatic diseases* 17, 44-49
24. Schiffmann S, Sandner J, Schmidt R et al. (2009) The selective COX-2 inhibitor celecoxib modulates sphingolipid synthesis. *J Lipid Res* 50, 32-40
25. Hla T and Kolesnick R (2014) C16:0-ceramide signals insulin resistance. *Cell metabolism* 20, 703-705
26. Park JW, Park WJ and Futerman AH (2014) Ceramide synthases as potential targets for therapeutic intervention in human diseases. *Biochimica et biophysica acta* 1841, 671-681
27. Liu X, Elojeimy S, Turner LS et al. (2008) Acid ceramidase inhibition: a novel target for cancer therapy. *Front Biosci* 13, 2293-2298
28. Tamehiro N, Zhou S, Okuhira K et al. (2008) SPTLC1 binds ABCA1 to negatively regulate trafficking and cholesterol efflux activity of the transporter. *Biochemistry* 47, 6138-6147
29. Tamehiro N, Mujawar Z, Zhou S et al. (2009) Cell polarity factor Par3 binds SPTLC1 and modulates monocyte serine palmitoyltransferase activity and chemotaxis. *J Biol Chem* 284, 24881-24890
30. Luo J, Deng ZL, Luo X et al. (2007) A protocol for rapid generation of recombinant adenoviruses using the AdEasy system. *Nat Protoc* 2, 1236-1247
31. Lee SY, Hong IK, Kim BR et al. (2015) Activation of sphingosine kinase 2 by endoplasmic reticulum stress ameliorates hepatic steatosis and insulin resistance in mice. *Hepatology* 62, 135-146
32. Yoo HH, Son J and Kim DH (2006) Liquid chromatography-tandem mass spectrometric determination of ceramides and related lipid species in cellular extracts. *J Chromatogr B Analyt Technol Biomed Life Sci* 843, 327-333

Figure 1

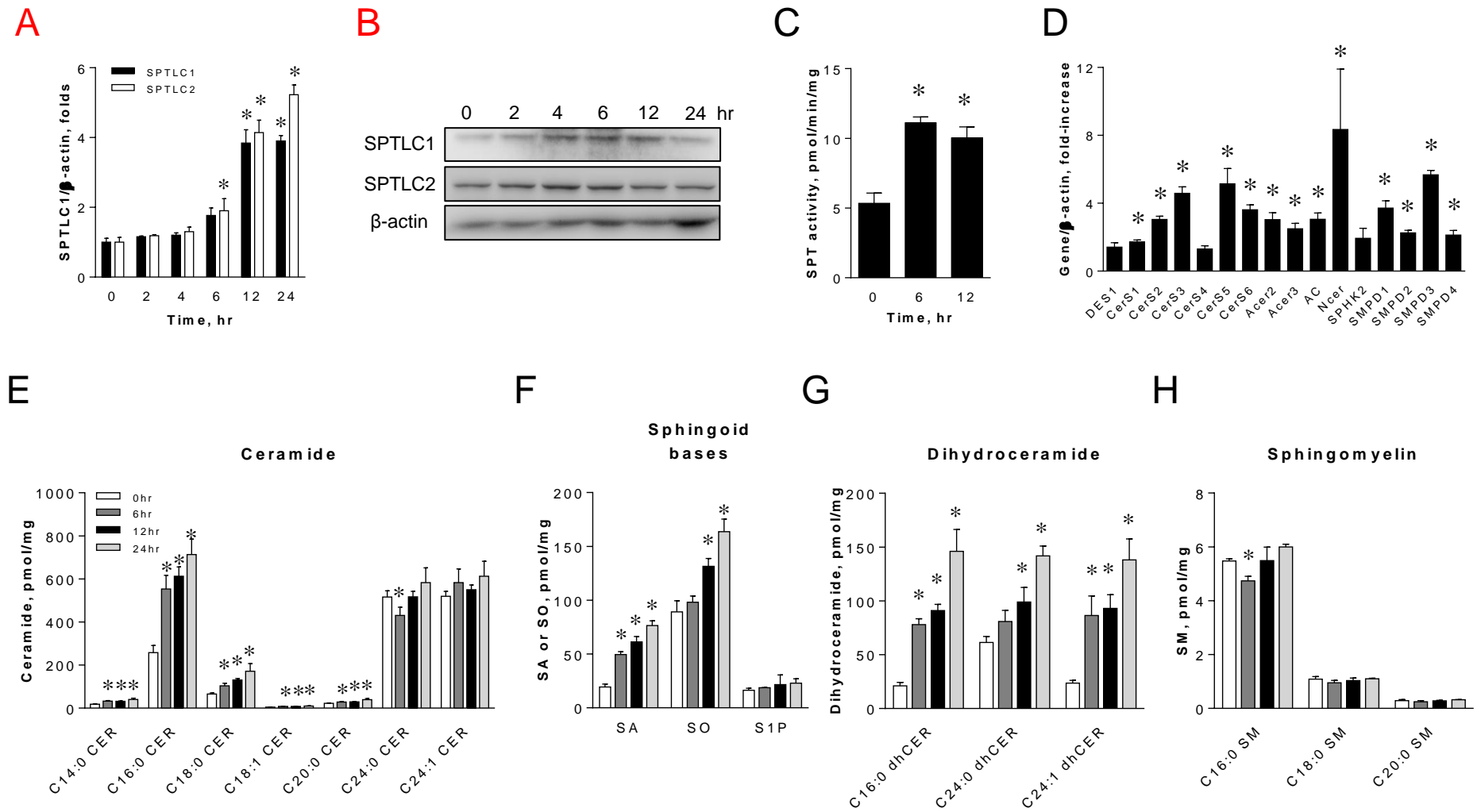


Figure 3

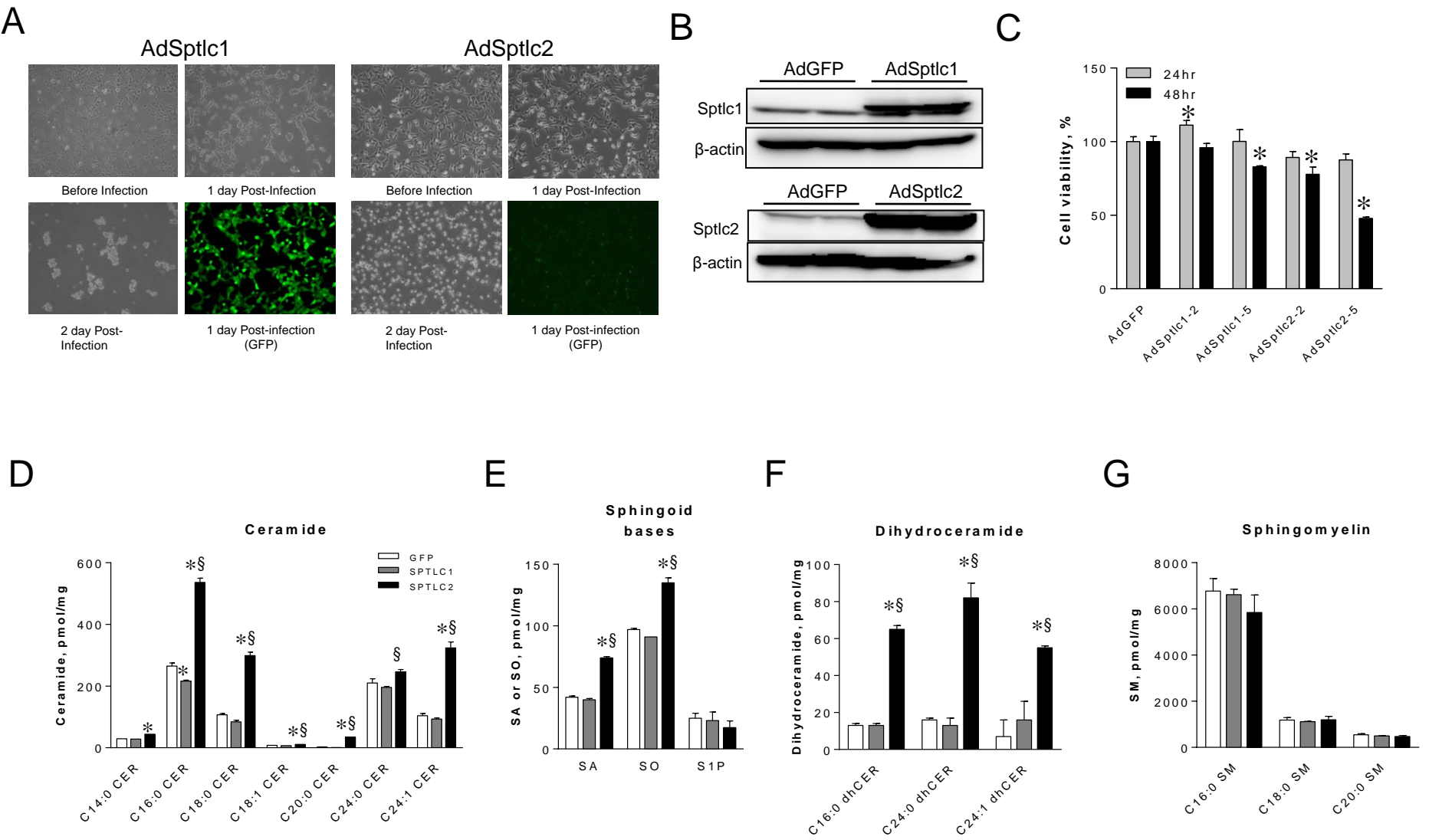
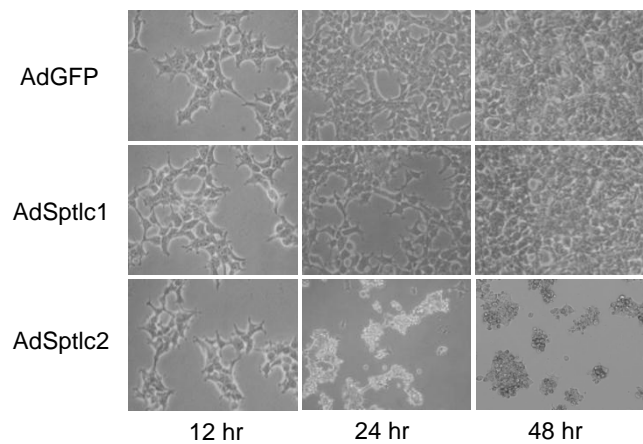
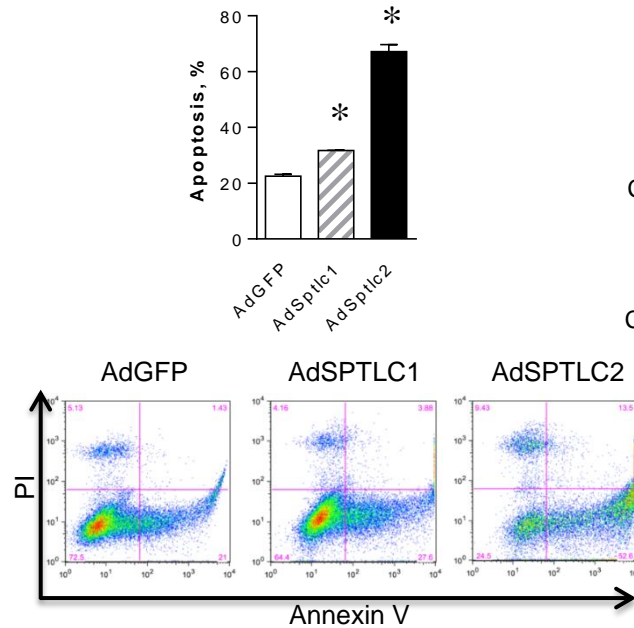


Figure 4

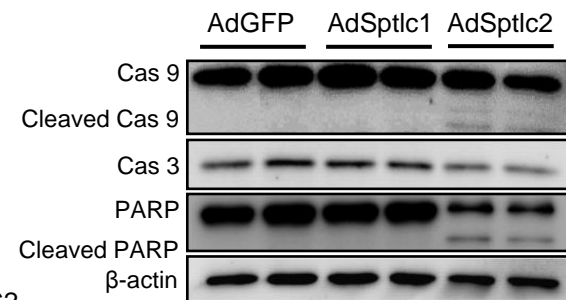
A



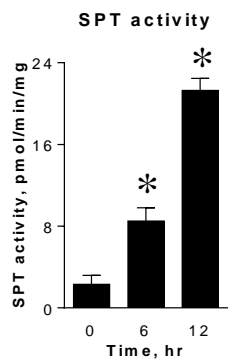
B



C



D



E

